Published OnlineFirst October 16, 2019; DOI: 10.1158/0008-5472.CAN-19-1405

Priority Report

Cancer Research

BRCA1 Deficiency Upregulates NNMT, Which Reprograms Metabolism and Sensitizes Ovarian Cancer Cells to Mitochondrial Metabolic Targeting Agents

Arun Kanakkanthara[1,2], Kiran Kurmi[2], Thomas L. Ekstrom[1], Xiaonan Hou[1], Emma R. Purfeerst[1], Ethan P. Heinzen[3], Cristina Correia[1], Catherine J. Huntoon[1], Daniel O'Brien[3], Andrea E. Wahner Hendrickson[1], Sean C. Dowdy[4], Hu Li[2], Ann L. Oberg[3], Taro Hitosugi[1,2], Scott H. Kaufmann[1,2], S. John Weroha[1], and Larry M. Karnitz[1,2]

Abstract

BRCA1 plays a key role in homologous recombination (HR) DNA repair. Accordingly, changes that downregulate BRCA1, including *BRCA1* mutations and reduced *BRCA1* transcription, due to promoter hypermethylation or loss of the BRCA1 transcriptional regulator CDK12, disrupt HR in multiple cancers. In addition, BRCA1 has also been implicated in the regulation of metabolism. Here, we show that reducing BRCA1 expression, either by CDK12 or BRCA1 depletion, led to metabolic reprogramming of ovarian cancer cells, causing decreased mitochondrial respiration and reduced ATP levels. BRCA1 depletion drove this reprogramming by upregulating nicotinamide N-methyltransferase (NNMT). Notably, the metabolic alterations caused by BRCA1 depletion and NNMT upregulation sensitized ovarian cancer cells to agents that inhibit mitochondrial metabolism (VLX600 and tigecycline) and to agents that inhibit glucose import (WZB117). These observations suggest that inhibition of energy metabolism may be a potential strategy to selectively target BRCA1-deficient high-grade serous ovarian cancer, which is characterized by frequent BRCA1 loss and NNMT overexpression.

Significance: Loss of BRCA1 reprograms metabolism, creating a therapeutically targetable vulnerability in ovarian cancer.

Introduction

Ovarian cancer is the leading cause of death from gynecologic malignancies. Patients with high-grade serous ovarian cancer (HGSOC), the most common and aggressive histotype, have a 5-year survival of only 20% to 30% (1). HGSOC is characterized by defects in homologous recombination (HR) repair that primarily arise from mutations in genes that encode *BRCA1*, *BRCA2*, and at least 11 other HR proteins. In a smaller subset of HGSOCs, HR defects reflect transcriptional repression of *BRCA1* resulting from hypermethylation of the *BRCA1* promoter or mutational inactivation of cyclin-dependent kinase 12 (CDK12), which regulates transcription of *BRCA1* and other genes involved in DNA repair (2, 3). Notably, deleterious *BRCA1* and *BRCA2* mutations are associated with better outcomes in patients treated with platinum-based therapies and PARP inhibitors due to the defects in HR repair (4).

Despite recent therapeutic advances seen with PARP inhibitors in HGSOC (5), new treatment options are still needed for this disease. One potential alternative target is reprogrammed tumor metabolism, which is emerging as a metabolic liability in many cancers (6, 7). Intriguingly, BRCA1 has recently been shown to regulate metabolism, and BRCA1 deficiency was shown to reduce mitochondrial oxygen consumption in breast cancer cells and skeletal muscle (8–10). These observations suggest that, in addition to its role in HR, BRCA1 also plays a key role in the regulation of mitochondrial metabolism. However, the mechanism by which BRCA1 loss reprograms tumor metabolism is unknown. Moreover, it is unclear whether BRCA1 deficiency also affects mitochondrial metabolism in HGSOC.

Nicotinamide N-methyltransferase (NNMT) has also emerged as a regulator of metabolism. NNMT catalyzes the transfer of methyl groups from S-adenosyl methionine (SAM) to nicotinamide, effectively increasing N1-methylnicotinamide levels and reducing SAM levels. Although it is not fully understood how NNMT expression affects cell metabolism, several studies have demonstrated that NNMT alters energy homeostasis in mice and that NNMT overexpression decreases oxygen consumption in adipocytes and hepatoma cells (11). Interestingly, NNMT is overexpressed in many tumors (12), including HGSOC (13, 14). In addition, depletion of NNMT blocks the proliferation of ovarian

[1]Department of Oncology, Mayo Clinic, Rochester, Minnesota. [2]Department of Molecular Pharmacology and Experimental Therapeutics, Mayo Clinic, Rochester, Minnesota. [3]Division of Biomedical Statistics and Informatics, Mayo Clinic, Rochester, Minnesota. [4]Division of Gynecologic Surgery, Mayo Clinic, Rochester, Minnesota.

Note: Supplementary data for this article are available at Cancer Research Online (http://cancerres.aacrjournals.org/).

Current address for Kiran Kurmi: Harvard Medical School, Boston MA 02115.

Corresponding Author: Larry M. Karnitz, Division of Oncology Research, Mayo Clinic, 200 First Street SW, Gonda 19-300, Rochester, MN 55905. Phone: 507-284-3124; Fax: 507-293-0107; E-mail: karnitz.larry@mayo.edu

Cancer Res 2019;79:5920–9

doi: 10.1158/0008-5472.CAN-19-1405

Published OnlineFirst October 16, 2019; DOI: 10.1158/0008-5472.CAN-19-1405

cancer cell lines selected to proliferate during metabolic stress induced by low glucose (13). Although these observations suggest that NNMT plays a role in ovarian cancer energy metabolism, it is not known whether NNMT affects sensitivity to metabolic inhibitors.

Here, we report that loss of BRCA1, induced by downregulation of either BRCA1 or CDK12, impairs mitochondrial respiration and reduces ATP levels. Notably, these metabolic changes are dependent on and phenocopied by NNMT overexpression, indicating that NNMT drives the metabolic remodeling. Consistent with the emerging idea that targeting mitochondrial dysfunction and/or tumor metabolism is a promising therapeutic approach to selectively kill metabolically defective tumor cells (6, 7), we find that BRCA1 depletion or NNMT overexpression confers sensivitity to agents that inhibit glucose transport and mitochondrial oxidative phosphorylation (OXPHOS), including agents that are in clinical trials as well as FDA-approved drugs that might be repurposed. Collectively, our data suggest that metabolic changes induced by *BRCA1* dysfunction and NNMT overexpression might be therapeutically exploited in BRCA1-deficient or NNMT-overexpressing HGSOC.

Materials and Methods

Cell lines, cell culture, and metabolism-targeting agents

OVCAR-8 and OVCAR-5 cells were kind gifts from D. Scudierio (NCI, NIH, Bethesda, MD). The PEA1 cell line was from Sigma-Aldrich. The *BRCA1*-mutant COV362 cell line was a gift from Robert van Waardenburg (University of Alabama at Birmingham, Birmingham, AL). The cells were cultured in RPMI-1640 medium (Corning) supplemented with 8% FBS (Millipore) and maintained in a humidified 37°C, 5% CO_2 incubator. All cells were authenticated by autosomal STR profiling (University of Arizona Genetics Core). All cell lines were free of *Mycoplasma* contamination as determined testing with a MycoAlert Mycoplasma Detection Kit (Lonza). VLX600 was obtained from Cayman Chemical. Tigecycline and WZB117 were obtained from Selleck Chemicals.

siRNAs and siRNA transfection

All siRNAs were purchased from Dharmacon. The siRNA sequences are listed in Supplementary Materials and Methods. siRNA (20 μL of 20 μmol/L siRNA/transfection) was mixed with 5–8 $\times$ 10^6 cells in 180 μL media in 4-mm cuvette and electroporated with a BTX ECM 830 electroporator with two, 280-volt, 10-msec pulses.

Plasmids, plasmid transfection, and stable cell line generation

A mammalian expression plasmid that encoded human NNMT fused to Myc and DDK tags at its C terminus was obtained from Origene (catalog no. RC200641). For the generation of stable NNMT-overexpressing OVCAR-8 cell lines, the NNMT-Myc-DDK plasmid or empty vector control was transfected (5 μg/transfection) into OVCAR-8 cells (8×10^6 cells/transfection) using a BTX ECM 830 electroporator (using a 4-mm cuvette with two, 280-volt, 10-msec pulses). Cells were plated in 10-cm dishes containing RPMI-1640 supplemented with 8% FBS and incubated for 48 hours. After G418 (2 mg/mL) was added, the cells were cultured for an additional 12 days, replenishing the selection medium every 3 days. G418-resistant clones were trypsinized using 0.25% Trypsin-EDTA (Life Technologies) and reseeded at 50 cells per dish into 15-cm dishes containing 2 mg/mL G418. After 10 days of culture, single colony clones were picked, expanded in 24-well plates containing complete medium plus G418. Seven to 10 days later, 10 empty vector or NNMT cell clones were isolated and assayed for NNMT by immunoblotting for each stably transfected cell line. To generate the SFB-BRCA1 mammalian expression plasmid, human full-length *BRCA1* cDNA (15) was subcloned into the pSFB vector that contains in-frame N-terminal S-peptide, FLAG, and streptavidin-binding peptide tags (16). For the generation of stable BRCA1-overexpressing COV362 cells, the SFB-BRCA1 plasmid or empty vector control plasmid was transfected (40 μg/transfection) into COV362 cells (10×10^6 cells/transfection), and after 48 hours, the cells were cultured for an additional 21 days with G418 (1 mg/mL), replenishing the selection medium every 3 days. The G418-resistant cells were used for subsequent experiments.

Immunoblotting

Forty-eight hours after siRNA transfection, cells were harvested and lysed in 50 mmol/L HEPES, pH 7.6, 150 mmol/L NaCl, 1 mmol/L EDTA, 1% Triton X-100, 10 mmol/L NaF, 30 mmol/L sodium pyrophosphate, 1 mmol/L Na_3VO_4, 10 mmol/L 2-glycerophosphate, 10 μg/mL leupeptin, 5 μg/mL aprotinin, 5 μg/mL pepstatin, and 20 mmol/L microcystin-LR. Immunoblotting was done using the following primary antibodies: mouse monoclonal CDK12, which was generated in our laboratory (Clone 1.11.1 B9, 1:100); mouse monoclonal BRCA1 (1:2,000, sc-6954, Santa Cruz Biotechnology); rabbit polyclonal BRCA2 (1:5,000, A303-434A, Bethyl Laboratories Inc.); mouse monoclonal NNMT (1:5,000, ab119758, Abcam); rabbit polyclonal RAD51 (1:2,000, PC-130, Calbiochem); rabbit polyclonal tubulin (1:1,000, 2144S, Cell Signaling Technology); rabbit monoclonal DYKDDDK (recognizes same sequence as FLAG, 1:1,000, 14793, Cell Signaling Technology); mouse monoclonal FLAG (F1804, Sigma); and mouse monoclonal HSP90 (1:1,000; D. Toft, Mayo Clinic, H9010). Secondary antibodies used were horseradish peroxidase–conjugated anti-mouse immunoglobulin G (1:10,000 for CDK12, 1:2,000 for BRCA1, and 1:20,000 for NNMT and HSP90, #7076S, Cell Signaling Technology) and anti-rabbit immunoglobulin G (1:5,000 for BRCA2 and DYKDDDK and 1:10,000 for RAD51 and tubulin, #7074S, Cell Signaling Technology).

Quantitative real-time PCR

Total RNA isolation from cells was performed using a miRNeasy Mini Kit (Qiagen) following the supplier's instructions. cDNA was synthesized from 1 μg of total RNA using oligo(dT) primers and SuperScript III reverse transcriptase (Thermo Fisher Scientific). Quantitative real-time PCR (qPCR) was performed in triplicate for each sample (25 ng cDNA template in a final volume of 20 μL) on a CFX96 real-time PCR system (Bio-Rad) using iTaq Universal SYBR Green Supermix (Bio-Rad). mRNA expression was normalized to GAPDH. The qPCR primers used are listed in Supplementary Materials and Methods.

Clonogenic assays

Two days after siRNA transfection, cells were seeded in 6-well plates at 300 cells/well for OVCAR-8 and 600 cells/well for PEA1 in triplicate and allowed to adhere overnight. The stable OVCAR-8-EV or OVCAR-8-Myc-DDK-NNMT cells were seeded at 300

Published OnlineFirst October 16, 2019; DOI: 10.1158/0008-5472.CAN-19-1405

cells/well. One day after plating, VLX600, tigecycline, or WZB117 was added at the indicated concentrations, and the cells were cultured for 8 to 10 days in the continued presence of the agents. Colonies were stained with Coomassie blue, and colonies of >50 cells were counted manually. Inhibition of colony formation was presented as percentage of colonies formed in corresponding untreated control.

Cell proliferation assay

Cell proliferation was assessed with the CyQUANT Cell Proliferation Assay Kit (Thermo Fisher Scientific). siRNA-transfected OVCAR-8 cells or stable OVCAR-8-EV or OVCAR-8-Myc-DDK-NNMT cells were plated at 4,000 cells/well in flat-bottom 96-well plates, and analyzed 24, 48, and 72 hours after plating following the supplier's instructions.

Chromatin immunoprecipitation assays

Cells (1×10^7) in 15-cm dishes were cross-linked with 1% formaldehyde in media for 10 minutes at room temperature, and the unreacted formaldehyde was quenched by adding 1/10 volume 1.25 mol/L glycine (pH 7.0). The cells were harvested by trypsinization, washed with PBS, and resuspended in cell lysis buffer (10 mmol/L Tris, HCl, pH 7.5, 10 mmol/L NaCl, 0.5% NP-40). After incubation on ice for 15 minutes, the chromatin fraction (pellet) was collected by centrifugation at $800 \times g$ for 5 minutes at 4°C, digested with micrococcal nuclease (2.5 U/mL; New England Biolabs) for 20 minutes at 37°C, and sonicated for 15 minutes. Aliquots of sheared chromatin were immunoprecipitated using protein G Dynabeads and 2 μg of mouse monoclonal BRCA1 (sc-6954, Santa Cruz Biotechnology) or mouse monoclonal FLAG (F1804, Sigma) antibodies. Normal mouse IgG (2 μg/ChIP, 0107-01, SouthernBiotech) was used as negative control. After immunoprecipitation, crosslinks were reversed by heating to 60°C, and immunoprecipitated DNA was purified using spin columns (catalog no. 11732676001, Roche). qPCR analysis of the immunoprecipitated and genomic input DNAs was performed using iQ SYBR Green Supermix (Bio-Rad). The following primers that amplify the *NNMT* promoter region were used: forward, 5′-CACTGCCTGTCTCTGACCAA-3′ and reverse, 5′-CAGGAGAACAGGGCTGAAAG-3′.

Mitochondrial DNA copy number analysis

OVCAR-8 cells (8×10^6) were transfected with nontargeting control, BRCA1, or CDK12 siRNAs. Two days after transfection, genomic DNA was extracted using the Wizard SV Genomic DNA Purification System (Promega). The relative number of copies of mitochondrial DNA were measured using the human mitochondrial DNA monitoring primer set (catalog no. 7246; Takara) and normalized using nuclear DNA content following the supplier's protocol.

ATP and ADP assays

Forty-eight hours after siRNA transfection, total ATP and ADP levels in the cells were measured using colorimetric ATP assay (catalog no. ab83355, Abcam) and ADP assay (catalog no. ab83359, Abcam) kits.

HGSOC tumor tissues

All HGSOC tumor tissues that were used in the *ex vivo* culture studies, mRNA expression studies, and protein expression studies were obtained in accord with the U.S. Common Rule after written informed consent was obtained under an active Mayo Clinic Institutional Review Board–approved banking protocol.

Ex vivo culture of HGSOC tumor tissues from PDX mouse models

All HGSOC tumor tissues were collected under an active protocol approved by the Mayo Clinic Institutional Review Board as described above. In compliance with the Health Insurance Portability and Accountability Act, all samples were first coded with a unique participant ID number with restricted access to the master key limited to authorized personnel of Mayo Clinic Ovarian Tumor Repository. To further protect patient confidentiality, patient-dervied xenograft (PDX) tumors were coded with a patient heterotransplant (PH) number for end-users of PDX models while the repository maintains a secure link back to participant ID numbers.

For short-term *ex vivo* monolayer cultures of tumor cells, HGSOC tissues from PDX mouse models were harvested, minced into 2- to 4-mm pieces, and dissociated using a Tumor Dissociation Kit (catalog no. 130-096-730, Miltenyi Biotec) following the supplier's protocol. The dissociated cells were washed 5 times with RPMI-1640 medium (Invitrogen) supplemented with 10% FBS (Invitrogen), 100 U/mL penicillin, and 100 U/mL streptomycin (Invitrogen). After resuspending in RPMI-1640 medium with 10% FBS without antibiotics, the cells were electroporated with control luciferase (Luc), nontargeting siRNA #3, BRCA1, or CDK12 siRNAs as described above. The cells were then plated in 24-well plates in RPMI-1640 supplemented with 10% FBS with antibiotics, cultured for 48 hours, and analyzed for ATP content using a colorimetric ATP assay (catalog no. ab83355, Abcam) and BRCA1 and CDK12 mRNA levels by qRT-PCR.

Correlation analyses of BRCA1 and CDK12 versus NNMT in patient and PDX tumors

All HGSOC tumor tissues were collected under an active protocol approved by the Mayo Clinic Institutional Review Board as described above. *CDK12*, *BRCA1*, and *NNMT* mRNA levels were obtained from an expression analysis in 98 HGSOC patient tumors and 127 nonoverlapping HGSOC PDX models grown in mice. All animal studies and procedures were reviewed and approved by the Mayo Clinic Institutional Animal Care and Use Committee. To assess the correlation between *NNMT* mRNA levels with *CDK12* and *BRCA1*, Spearman correlation analysis was performed.

Seahorse assay

Twenty-four hours after siRNA transfection, OVCAR-8 or PEA1 cells were plated at 8,000 or 7,000 cells/well, respectively, onto Seahorse 8-well XFp cell culture miniplates and allowed to grow for another 24 hours before being assayed for oxygen consumption rate (OCR) and extracellular acidification rate (ECAR) on a Seahorse XFp extracellular flux analyzer (Seahorse Bioscience, Agilent Technologies). One hour prior to the start of the assay, cells were washed and changed to Seahorse XF base assay medium supplemented with 2 mmol/L L-glutamine and 10 mmol/L glucose, adjusted to pH 7.4, and incubated in a 37°C non-CO_2 incubator. OCR was measured using the Seahorse XFp Cell Mito Stress Test Kit (Agilent Technologies)

Published OnlineFirst October 16, 2019; DOI: 10.1158/0008-5472.CAN-19-1405

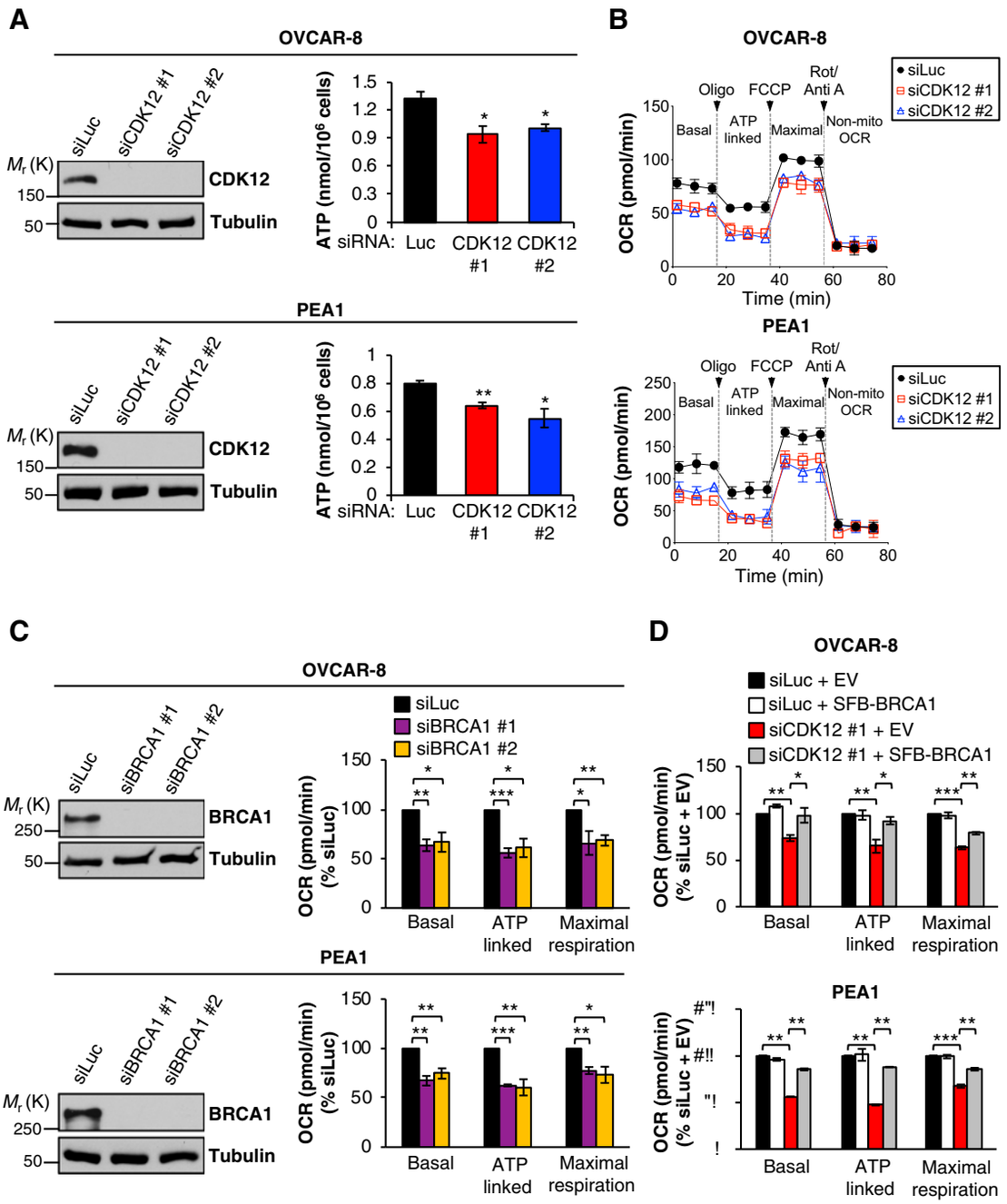

Figure 1.

CDK12 depletion downregulates BRCA1, which causes decreased ATP levels and suppresses mitochondrial respiration. **A,** Analysis of ATP levels in CDK12-depleted cells. OVCAR-8 (top) and PEA1 (bottom) cells were transfected with control luciferase (siLuc) or CDK12 siRNAs (siCDK12 #1 and siCDK12 #2). Forty-eight hours after transfection, ATP levels were measured (right), and CDK12 and tubulin levels were analyzed by immunoblotting (left). **B,** Effect of CDK12 depletion on OCR. OVCAR-8 or PEA1 cells were transfected with control siLuc or CDK12 siRNAs. Forty-eight hours later, OCRs were measured under basal conditions, following the sequential additions of oligomycin, FCCP, and rotenone/antimycin A using a Seahorse XFp extracellular flux analyzer. Data are representative of three independent experiments. **C,** BRCA1 depletion also disrupts OCR. OVCAR-8 and PEA1 cells were transfected with control siLuc or BRCA1 siRNAs (siBRCA1 #1 and siBRCA1 #2). Forty-eight hours later, BRCA1 and tubulin were analyzed by immunoblotting (left), and OCR was measured as described in **B** (right). **D,** Ectopic BRCA1 expression rescues the OCR defect induced by BRCA1. OVCAR-8 (top) and PEA1 (bottom) cells were transfected with siLuc or CDK12 siRNAs plus empty vector (EV) or SFB-BRCA1 plasmid (SFB-BRCA1). OCR was measured as described in **B**. Data, means ± SEM; $n = 3$ independent experiments. *, $P < 0.05$; **, $P < 0.01$; ***, $P < 0.001$, unpaired t test.

Published OnlineFirst October 16, 2019; DOI: 10.1158/0008-5472.CAN-19-1405

under basal conditions and after the sequential addition of 1 μmol/L oligomycin, 0.5 μmol/L carbonyl cyanide p-trifluoromethoxyphenylhydrazone (FCCP), and 0.5 μmol/L rotenone and antimycin A. ECAR was measured under basal conditions and after sequential injections of 10 mmol/L glucose, 2.5 μmol/L oligomycin and 50 mmol/L 2-deoxy-glucose. OCR and ECAR measurements were taken at three time points before and after the addition of each inhibitor. Experiments were repeated three times, with 2 or more samples per experimental point.

Accession number

The RNA sequencing (RNA-seq) count data have been deposited in the Gene Expression Omnibus database under accession number GSE138288.

Results and Discussion

CDK12 depletion disrupts mitochondrial metabolism, reducing respiration but not glycolysis

While assessing how loss of CDK12 affects ovarian cancer cells, we observed that CDK12 depletion reduced ATP levels in OVCAR-8 and PEA1 cells (Fig. 1A; Supplementary Fig. S1A), with corresponding increases in ADP levels (Supplementary Fig. S1B). Because ATP is produced primarily by OXPHOS or glycolysis (17), we profiled the metabolic activity of these cells using extracellular flux analyses to determine whether CDK12 depletion affected either process. These studies showed that ECAR, an indicator of glycolysis, was not reduced by CDK12 depletion (Supplementary Fig. S1C). In contrast, OCR, an indicator of OXPHOS, was reduced under basal conditions (Fig. 1B) as well as after treatment with oligomycin, an inhibitor of ATP synthase; FCCP, an uncoupler of mitochondrial oxidative phosphorylation; and rotenone and antimycin A, two inhibitors of mitochondrial electron transport complexes I and II, respectively (18). These findings demonstrate that CDK12 depletion reprograms mitochondrial metabolism, leading to reduced OCR and ATP production.

Metabolic reprogramming induced by CDK12 depletion is phenocopied by BRCA1 depletion

Studies from our laboratory and others have shown that CDK12 depletion reduces BRCA1 expression (2, 3). Because BRCA1 defects have previously been shown to reduce mitochondrial oxygen consumption in breast cancer cells (9), we asked whether the mitochondrial respiration defects induced by CDK12 loss may actually be caused by loss of BRCA1. Consistent with this possibility, BRCA1 depletion also reduced OCR (Fig. 1C) and ATP production (Supplementary Fig. S1A) without disrupting glycolysis (Supplementary Fig. S2A and S2B). Similarly, depletion of CDK12 and BRCA1 reduced ATP levels in *ex vivo*–cultured HGSOC patient-derived xenografts (Supplementary Fig. S2C and S2D), indicating that this effect was not unique to cell lines. In agreement with these findings, BRCA1 reexpression in BRCA1-deficient COV362 ovarian cancer cells increased OCR (Supplementary Fig. S2E). The reduced OCR and ATP levels caused by CDK12 or BRCA1 depletion were not the result of reduced mitochondrial number, as determined by mitochondrial DNA copy number (Supplementary Fig. S2F), suggesting that they stem from decreased flux through electron transport complexes rather than a decrease in mitochondria. Taken together, these results demonstrate that BRCA1 regulates OCR and ATP levels in ovarian cancer cells.

Finally, we addressed whether the OCR reduction caused by CDK12 depletion was driven by the corresponding loss of BRCA1. This analysis showed that reexpression of exogenous BRCA1 in CDK12-depleted cells restored OCR in CDK12-depleted cells (Fig. 1D; Supplementary Fig. S2G and S2H), thus demonstrating that the BRCA1 loss caused by CDK12 depletion drives metabolic reprogramming.

Disabling HR does not cause the mitochondrial dysfunction induced by BRCA1 depletion

Because BRCA1 plays a central role in HR DNA repair (19), we next asked whether an HR defect induced by loss of other HR proteins would similarly cause the mitochondrial defect induced by BRCA1 depletion. In contrast to what was observed with BRCA1 depletion, depletion of BRCA2, a key participant in HR, did not cause defects in OCR (Supplementary Fig. S3A) but did disrupt HR, as shown by increased sensitivity to the PARP inhibitor olaparib (Supplementary Fig. S3B). Similar results were seen with RAD51 depletion, which did not affect OCR but did sensitize to olaparib (Supplementary Fig. S3C and S3D). Taken together, these results suggest that the role of BRCA1 in metabolism is independent of its role in HR and support a model in which BRCA1 deficiency reprograms mitochondrial metabolism in ovarian cancer.

Upregulation of NNMT drives the metabolic alteration caused by BRCA1 depletion

To gain insight into how CDK12 and BRCA1 depletion affected mitochondrial respiration, we analyzed an RNA-seq dataset from control and CDK12-depleted OVCAR-8 cells (Supplementary Table S1). Consistent with previously published RNA-seq analyses (3, 20), CDK12 depletion altered the expression of genes involved in DNA replication, DNA repair, RNA processing, and RNA splicing (Supplementary Table S1). However, we also noticed that NNMT mRNA levels were increased approximately 4-fold in the CDK12-depleted cells (Supplementary Table S1). Because NNMT has been implicated in mitochondrial energy metabolism (11, 13, 21), and it is frequently overexpressed in multiple cancers (12), including HGSOC (13, 14), we asked (i) whether BRCA1 levels affected NNMT levels in cell lines and human tumors and (ii) whether NNMT overexpression could drive the decrease in OCR.

To explore these questions, we first demonstrated that two independent BRCA1 siRNAs, which target two different exons and suppress expression of multiple forms of BRCA1 mRNAs (Supplementary Fig. S4A and S4B), increased NNMT mRNA and protein levels in multiple ovarian cancer cell lines (Fig. 2A; Supplementary Fig. S4C). Consistent with the cell line studies, NNMT mRNA and BRCA1 mRNA levels were inversely correlated in HGSOC patient tumors and in tumors grown in PDX models (Fig. 2B, left two panels). Similarly, NNMT protein levels were also inversely correlated with *BRCA1* mRNA and CDK12 protein levels in HGSOC tumors (Fig. 2B, right two panels; Supplementary Table S2). Second, to determine whether BRCA1 loss drives these metabolic effects by upregulating NNMT, we codepleted NNMT and BRCA1 and found that

Published OnlineFirst October 16, 2019; DOI: 10.1158/0008-5472.CAN-19-1405

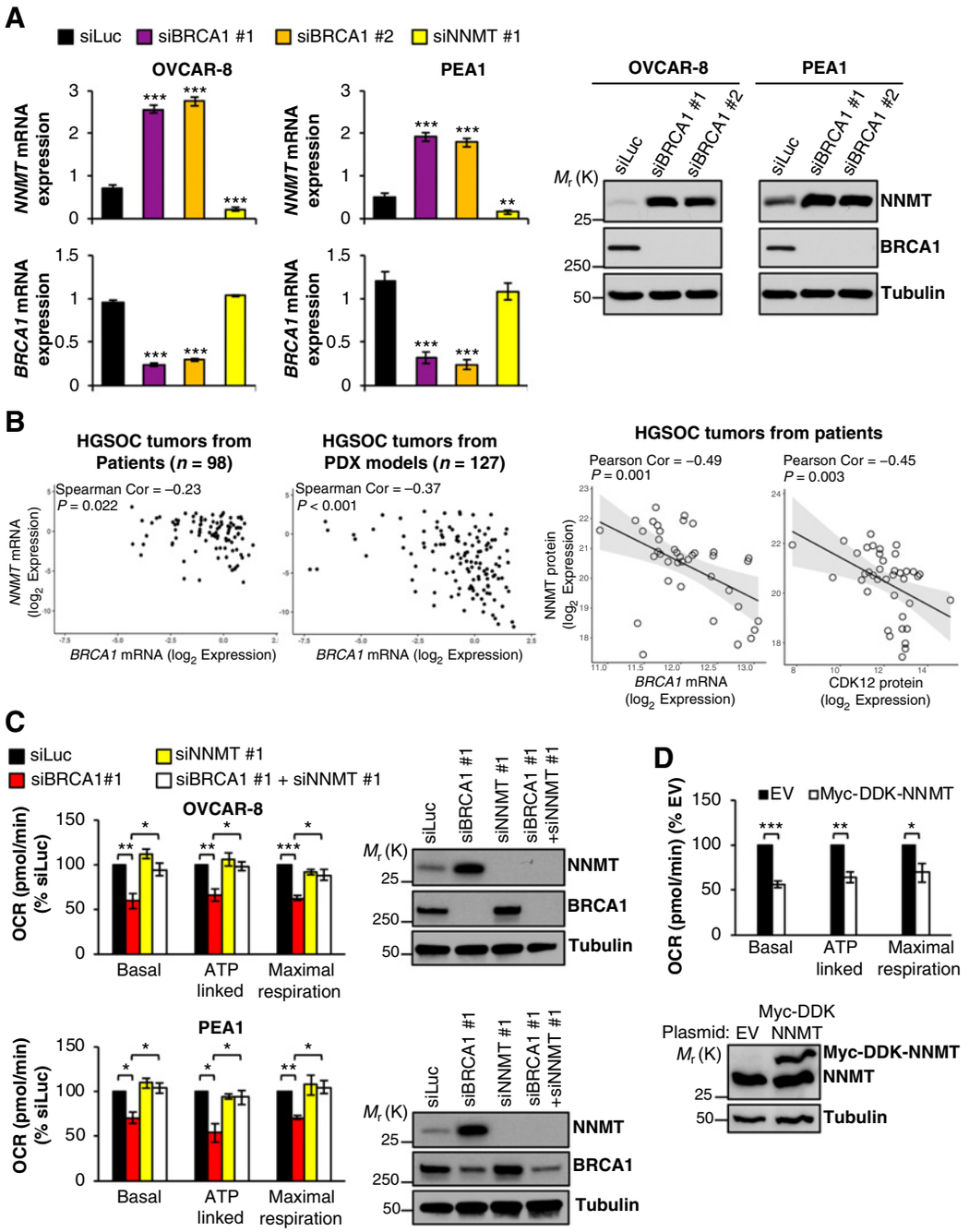

Figure 2.

BRCA1 depletion induces NNMT upregulation, which causes decreased OCR. **A,** OVCAR-8 and PEA1 cells were transfected with control luciferase (siLuc), BRCA1, or NNMT siRNAs. Forty-eight hours later, the cells were analyzed by qPCR for *NNMT* and *BRCA1* mRNA levels, which were expressed relative to *GAPDH* mRNA levels as an internal control (left) and immunoblotted for NNMT, BRCA1, and tubulin (right). **B,** BRCA1 and CDK12 mRNA and protein levels were inversely correlated with NNMT mRNA and protein. Left two panels, scatter plots of *NNMT* mRNA expression as a function of *BRCA1* and *CDK12* mRNA expression in HGSOC tumors from patients and PDX models. Right two panels, scatter plots of NNMT protein as a function of *BRCA1* mRNA and CDK12 protein levels in HGSOC tumors from patients. Spearman or Pearson correlations are shown in the images. **C,** Codepletion of NNMT reverses the OCR defect induced by BRCA1 depletion. OVCAR-8 (top) and PEA1 (bottom) cells were transfected with siLuc, BRCA1, or NNMT siRNAs individually or cotransfected with BRCA1 and NNMT siRNAs. OCR was measured as described in Fig. 1B and NNMT, BRCA1, and tubulin levels were measured by immunoblotting. **D,** NNMT overexpression phenocopies the OCR defect induced by BRCA1 depletion. OVCAR-8 cells were transiently transfected with empty vector (EV) or a plasmid that expresses Myc-DDK-tagged NNMT. After 24 hours, OCR was analyzed as described in Fig. 1B and cells were immunoblotted for NNMT and tubulin. Data, means ± SEM; $n = 3$ independent experiments. *, $P < 0.05$; **, $P < 0.01$; ***, $P < 0.001$, unpaired *t* test.

Published OnlineFirst October 16, 2019; DOI: 10.1158/0008-5472.CAN-19-1405

NNMT depletion reversed the OCR defect caused by BRCA1 depletion (Fig. 2C). Moreover, we also found that BRCA1, which is known to regulate gene transcription, occupies the *NNMT* promoter (Supplementary Fig. S4D and S4E). Finally, we observed that transient overexpression of NNMT reduced OCR (Fig. 2D). Taken together, these results demonstrate that BRCA1 occupies the *NNMT* promoter and regulates NNMT expression. In addition, these results show that NNMT is both necessary and sufficient to reprogram mitochondrial metabolism in ovarian cancer cells.

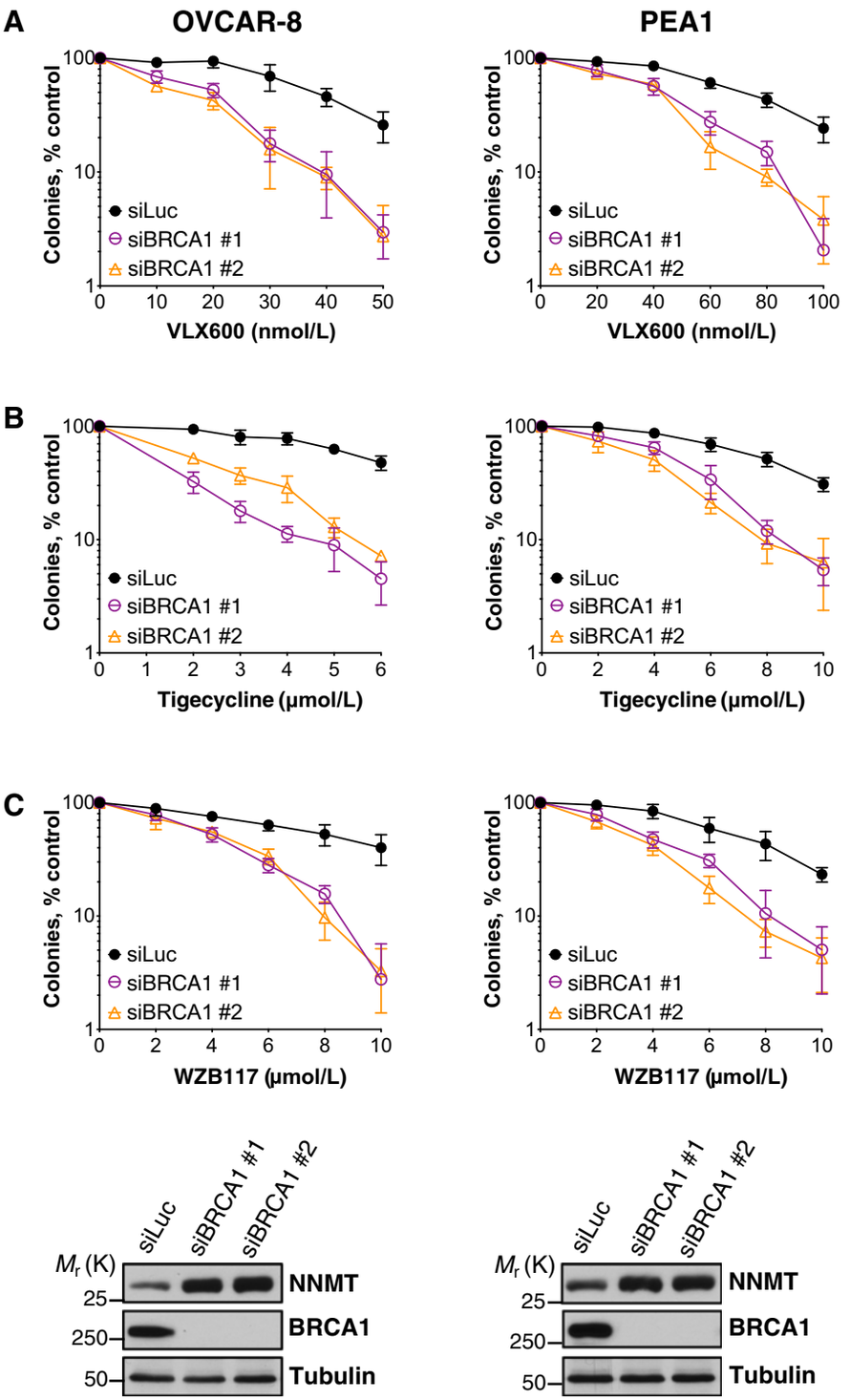

Figure 3.
BRCA1 depletion sensitizes ovarian cancer cells to agents that disrupt metabolism. **A–C,** OVCAR-8 and PEA1 cells were transfected with control luciferase (siLuc) or BRCA1 siRNAs. Forty-eight hours later, the cells were trypsinized, immunoblotted for BRCA1 and tubulin (bottom), and subjected to colony formation assays. The indicated concentrations of VLX600 (**A**), tigecycline (**B**), or WZB117 (**C**) were added 12 hours after plating, and the cells were cultured for 8 to 10 days to allow colony formation. Data are representative of three independent experiments. Error bars, means ± SEM of three technical replicates in the representative experiment.

Published OnlineFirst October 16, 2019; DOI: 10.1158/0008-5472.CAN-19-1405

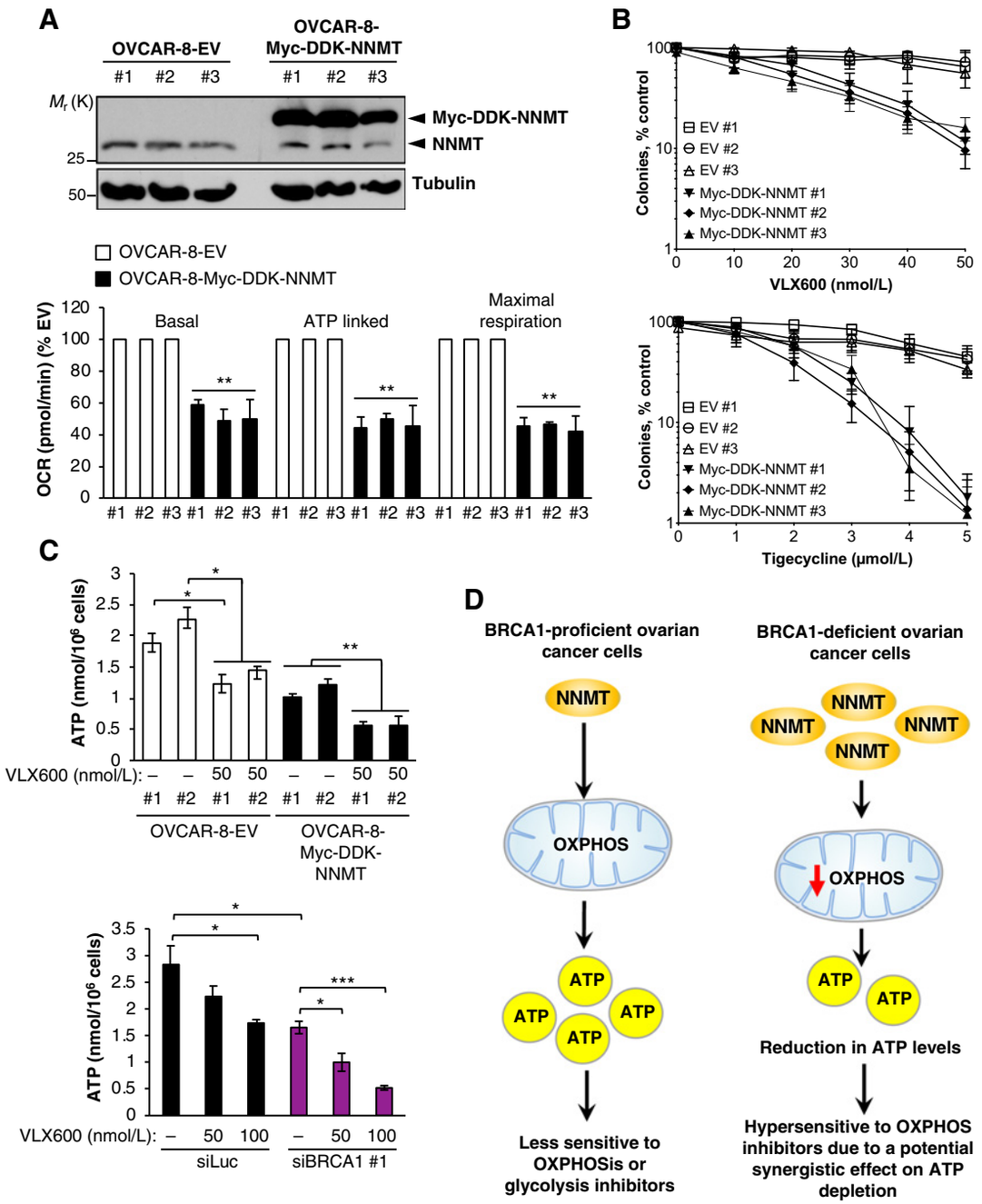

Figure 4.

NNMT overexpression sensitizes ovarian cancer cells to agents that disrupt metabolism. **A** and **B,** Clones of OVCAR-8 cells stably transfected with empty vector (pcDNA3) or the Myc-DDK-NNMT expression plasmid were subjected to immunoblotting for NNMT and tubulin (**A**, top), examined for OCR as described in Fig. 1B (**A**, bottom), and treated with VLX600 (**B**, top) or tigecycline (**B**, top), which was added 12 hours after plating the cells. The cells were cultured for 8 to 10 days to allow colony formation. Data in **B** are representative of three independent experiments. Error bars, means ± SEM of three technical replicates for each data point in the representative experiment. **C,** VLX600 further reduces ATP levels in NNMT-overexpressing cells (top) and BRCA1-depleted cells (bottom). Stable clones of the OVCAR-8-EV or the OVCAR-8-Myc-DDK-NNMT cells were treated with 50 nmol/L VLX600 for 24 hours, and OCR was measured as described in Fig. 1B (top). Control luciferase (siLuc)- or BRCA1 siRNA-transfected OVCAR-8 cells were treated with indicated concentrations of VLX600 for 24 hours and OCR was measured (bottom). **D,** Model for the increased cytotoxic effect of metabolic inhibitors in BRCA1-deficient cells. Left, in BRCA1-proficient cells, low NNMT levels lead to higher ATP levels so that these cells are less sensitive to metabolic inhibitors. Right, in BRCA1-deficient cells, NNMT levels are increased, leading to reduction in OXPHOS and ATP levels. These cells are more sensitive to OXPHOS inhibitors, because they are already metabolically stressed and unable to meet their energy demands when challenged with inhibitors that further reduce ATP levels. Data, means ± SEM; $n = 3$ independent experiments; *, $P < 0.05$; **, $P < 0.01$, unpaired t test.

Published OnlineFirst October 16, 2019; DOI: 10.1158/0008-5472.CAN-19-1405

BRCA1 depletion sensitizes ovarian cancer cells to mitochondrial metabolic targeting agents

Because BRCA1 depletion disrupted mitochondrial respiration and reduced ATP levels (Fig. 1C; Supplementary Figs. S1A and S2C), we reasoned that BRCA1-deficient cells would be more sensitive to agents that cause additional metabolic stress. To test this possibility, we assessed the effect of several small molecules that inhibit energy metabolism. These include: (i) VLX600, an iron chelator that targets metabolically compromised tumors by causing mitochondrial dysfunction and inhibiting mitochondrial respiration (7); (ii) tigecycline, an FDA-approved antibiotic that inhibits mitochondrial protein translation (22); and (iii) WZB117, which inhibits the glucose transporter GLUT1 and reduces intracellular ATP levels (23). As shown in Fig. 3, BRCA1 depletion sensitized OVCAR-8 and PEA1 cells to all three agents (Fig. 3A–C) and upregulated NNMT (Fig. 3, bottom). Consistent with the observation that loss of BRCA2 and RAD51 did not disrupt OCR (Supplementary Fig. S3A and S3C), depletion of these HR proteins did not sensitize cells to OXPHOS inhibition (but did sensitize to the PARP inhibitor olaparib; Supplementary Fig. S5A and S5B). These findings demonstrate that the metabolic reprogramming induced by BRCA1 loss sensitizes ovarian cancer cells to agents that disrupt energy metabolism and further indicate that BRCA1 regulation of metabolism is unrelated to its role in HR.

NNMT overexpression sensitizes ovarian cancer cells to mitochondrial metabolic targeting agents

Because mitochondrial metabolic defects induced by BRCA1 depletion occurred through NNMT upregulation (Fig. 2), we next asked whether NNMT overexpression was sufficient to sensitize ovarian cancer cells to mitochondrial metabolic targeting agents. To assess this possibility, we created three clones of OVCAR-8 cells that stably overexpress NNMT (Fig. 4A). As was seen with BRCA1 depletion, NNMT overexpression reduced OCR (Fig. 4A) and ATP levels (Supplementary Fig. S6A). Moreover, CDK12 or BRCA1 depletion did not further reduce ATP levels when NNMT was overexpressed (Supplementary Fig. S6A), indicating that reduced ATP levels caused by BRCA1 depletion are driven primarily by NNMT overexpression. Notably, these NNMT-induced metabolic changes were not due to reduced proliferation rate (Supplementary Fig. S6B), although BRCA1 depletion did reduce proliferation (Supplementary Fig. S6C), likely because BRCA1 has additional effects on cell proliferation (24). Consistent with reduced OCR and ATP levels (Fig. 4A; Supplementary Fig. S6A), NNMT overexpression sensitized the cells to mitochondrial metabolic targeting agents (Fig. 4B). These results demonstrate that NNMT upregulation reprograms metabolism and sensitizes ovarian cancer cells to agents that target mitochondrial metabolism without reducing proliferation.

In an attempt to understand why OXPHOS inhibitors were more cytotoxic in BRCA1-depleted and NNMT-overexpressing cells, we assessed the impact of an OXPHOS inhibitor on ATP levels in BRCA1-depleted and NNMT overexpressing OVCAR-8 cells, which already have compromised ATP levels (Supplementary Figs. S1A, S2C, and S6A). Consistent with the previous reports showing that VLX600 reduced ATP levels (7), we observed a further reduction in ATP in BRCA1-depleted as well as in NNMT-overexpressing cells (Fig. 4C). These results suggest that OXPHOS inhibitors are more toxic in cells with reduced levels of OXPHOS, possibly due to the additional metabolic stress imposed by agents such as VLX600 and other OXPHOS inhibitors (Fig. 4D).

Summary

In summary, we demonstrated here that BRCA1 deficiency, via its ability to upregulate NNMT, reprograms metabolism by reducing mitochondrial respiration. We also showed that this metabolic reprogramming sensitizes ovarian cancer cells to small molecules that disrupt energy metabolism. Interestingly, the concentrations of VLX600 that are selectively cytotoxic to BRCA1-deficient and NNMT-overexpressing cells are readily achieved in patients treated with this agent. For example, a phase I trial of VLX600 as a single agent found plasma C_{max} concentrations of 1 to 2 μmol/L in humans (25), well above the 30 to 100 nmol/L concentrations used in the current studies (Fig. 3). Because BRCA1 dysfunction and NNMT overexpression are common features of many cancers (12), including HGSOC (13, 14), our findings suggest that metabolic vulnerabilities created by these tumor-associated alterations might be common and might be therapeutically targeted by agents that are FDA approved or have been in clinical trials.

Disclosure of Potential Conflicts of Interest

A. Kanakkanthara and L.M. Karnitz are co-inventors on a provisional patent application related to the findings in this article. No potential conflicts of interest were disclosed by the other authors.

Authors' Contributions

Conception and design: A. Kanakkanthara, X. Hou, S.C. Dowdy, S.J. Weroha, L.M. Karnitz

Development of methodology: K. Kurmi, T.L. Ekstrom, X. Hou, D. O'Brien, S.J. Weroha, L.M. Karnitz

Acquisition of data (provided animals, acquired and managed patients, provided facilities, etc.): A. Kanakkanthara, K. Kurmi, T.L. Ekstrom, C.J. Huntoon, D. O'Brien, A.E. Wahner Hendrickson, S.H. Kaufmann, S.J. Weroha, L.M. Karnitz

Analysis and interpretation of data (e.g., statistical analysis, biostatistics, computational analysis): A. Kanakkanthara, E.P. Heinzen, C. Correia, D. O'Brien, A.E. Wahner Hendrickson, S.C. Dowdy, H. Li, A.L. Oberg, T. Hitosugi, S.J. Weroha, L.M. Karnitz

Writing, review, and/or revision of the manuscript: A. Kanakkanthara, E.R. Purfeerst, E.P. Heinzen, C. Correia, C.J. Huntoon, D. O'Brien, A.E. Wahner Hendrickson, S.C. Dowdy, A.L. Oberg, S.H. Kaufmann, S.J. Weroha, L.M. Karnitz

Administrative, technical, or material support (i.e., reporting or organizing data, constructing databases): E.P. Heinzen, D. O'Brien, L.M. Karnitz

Study supervision: A. Kanakkanthara, X. Hou, S.J. Weroha, L.M. Karnitz

Acknowledgments

This work was supported by NIH (R01 CA194498 to L.M. Karnitz), Mayo Clinic Ovarian Cancer SPORE (P50 CA136393 to S.H. Kaufmann), a Mayo Clinic Ovarian Cancer SPORE Career Enhancement Award (P50 CA136393 to A. Kanakkanthara), a Foundation for Women's Cancer Genentech Ovarian Cancer Young Investigator Career Development Award (to A. Kanakkanthara), a Wallace and Evelyn Simmers Career Development Award for Ovarian Cancer Research (to A. Kanakkanthara), and an infrastructure grant from the Minnesota Partnership for Biotechnology & Medical Genomics (to S.H. Kaufmann).

Received May 3, 2019; revised September 5, 2019; accepted October 9, 2019; published first October 16, 2019.

Published OnlineFirst October 16, 2019; DOI: 10.1158/0008-5472.CAN-19-1405

References

1. Bowtell DD, Bohm S, Ahmed AA, Aspuria PJ, Bast RC Jr, Beral V, et al. Rethinking ovarian cancer II: reducing mortality from high-grade serous ovarian cancer. Nat Rev Cancer 2015;15:668–79.
2. Joshi PM, Sutor SL, Huntoon CJ, Karnitz LM. Ovarian cancer-associated mutations disable catalytic activity of CDK12, a kinase that promotes homologous recombination repair and resistance to cisplatin and poly(ADP-ribose) polymerase inhibitors. J Biol Chem 2014;289:9247–53.
3. Blazek D, Kohoutek J, Bartholomeeusen K, Johansen E, Hulinkova P, Luo Z, et al. The cyclin K/Cdk12 complex maintains genomic stability via regulation of expression of DNA damage response genes. Genes Dev 2011;25:2158–72.
4. Lord CJ, Ashworth A. BRCAness revisited. Nat Rev Cancer 2016;16:110–20.
5. Morgan RD, Clamp AR, Evans DGR, Edmondson RJ, Jayson GC. PARP inhibitors in platinum-sensitive high-grade serous ovarian cancer. Cancer Chemother Pharmacol 2018;81:647–58.
6. Vander Heiden MG. Targeting cancer metabolism: a therapeutic window opens. Nat Rev Drug Discov 2011;10:671–84.
7. Zhang XN, Fryknas M, Hernlund E, Fayad W, De Milito A, Olofsson MH, et al. Induction of mitochondrial dysfunction as a strategy for targeting tumour cells in metabolically compromised microenvironments. Nat Commun 2014;5:3295.
8. Jackson KC, Gidlund EK, Norrbom J, Valencia AP, Thomson DM, Schuh RA, et al. BRCA1 is a novel regulator of metabolic function in skeletal muscle. J Lipid Res 2014;55:668–80.
9. Privat M, Radosevic-Robin N, Aubel C, Cayre A, Penault-Llorca F, Marceau G, et al. BRCA1 induces major energetic metabolism reprogramming in breast cancer cells. PLoS One 2014;9:e102438.
10. Jackson KC, Tarpey MD, Valencia AP, Inigo MR, Pratt SJ, Patteson DJ, et al. Induced Cre-mediated knockdown of Brca1 in skeletal muscle reduces mitochondrial respiration and prevents glucose intolerance in adult mice on a high-fat diet. FASEB J 2018;32:3070–84.
11. Kraus D, Yang Q, Kong D, Banks AS, Zhang L, Rodgers JT, et al. Nicotinamide N-methyltransferase knockdown protects against diet-induced obesity. Nature 2014;508:258–62.
12. Pissios P. Nicotinamide N-methyltransferase: more than a vitamin B3 clearance enzyme. Trends Endocrin Met 2017;28:340–53.
13. Kanska J, Aspuria PJP, Taylor-Harding B, Spurka L, Funari V, Orsulic S, et al. Glucose deprivation elicits phenotypic plasticity via ZEB1-mediated expression of NNMT. Oncotarget 2017;8:26200–20.
14. Eckert MA, Coscia F, Chryplewicz A, Chang JW, Hernandez KM, Pan S, et al. Proteomics reveals NNMT as a master metabolic regulator of cancer-associated fibroblasts. Nature 2019;569:723–8.
15. Wang A, Schneider-Broussard R, Kumar AP, MacLeod MC, Johnson DG. Regulation of BRCA1 expression by the Rb-E2F pathway. J Biol Chem 2000;275:4532–6.
16. Chini CC, Chen J. Repeated phosphopeptide motifs in human Claspin are phosphorylated by Chk1 and mediate Claspin function. J Biol Chem 2006;281:33276–82.
17. Moreno-Sanchez R, Marin-Hernandez A, Saavedra E, Pardo JP, Ralph SJ, Rodriguez-Enriquez S. Who controls the ATP supply in cancer cells? Biochemistry lessons to understand cancer energy metabolism. Int J Biochem Cell B 2014;50:10–23.
18. Perry SW, Norman JP, Barbieri J, Brown EB, Gelbard HA. Mitochondrial membrane potential probes and the proton gradient: a practical usage guide. Biotechniques 2011;50:98–115.
19. Konstantinopoulos PA, Ceccaldi R, Shapiro GI, D'Andrea AD. Homologous recombination deficiency: exploiting the fundamental vulnerability of ovarian cancer. Cancer Discov 2015;5:1137–54.
20. Liang K, Gao X, Gilmore JM, Florens L, Washburn MP, Smith E, et al. Characterization of human CDK12 and CDK13 complexes in CTD phosphorylation, gene transcription and RNA processing. Mol Cell Biol 2015;35:928–38.
21. Ulanovskaya OA, Zuhl AM, Cravatt BF. NNMT promotes epigenetic remodeling in cancer by creating a metabolic methylation sink. Nat Chem Biol 2013;9:300–6.
22. Jia XF, Gu ZF, Chen WM, Jiao JB. Tigecycline targets nonsmall cell lung cancer through inhibition of mitochondrial function. Fund Clin Pharmacol 2016;30:297–306.
23. Liu Y, Cao YY, Zhang WH, Bergmeier S, Qian YR, Akbar H, et al. A small-molecule inhibitor of glucose transporter 1 downregulates glycolysis, induces cell-cycle arrest, and inhibits cancer cell growth *in vitro* and *in vivo*. Mol Cancer Ther 2012;11:1672–82.
24. Deng CX. BRCA1: cell cycle checkpoint, genetic instability, DNA damage response and cancer evolution. Nucleic Acids Res 2006;34:1416–26.
25. Mody K, Mansfield AS, Vemireddy L, Nygren P, Gulbo J, Borad M. A phase I study of the safety and tolerability of VLX600, an iron chelator, in patients with refractory advanced solid tumors. Invest New Drugs 2019;37:684–92.

Published OnlineFirst October 16, 2019; DOI: 10.1158/0008-5472.CAN-19-1405

Cancer Research
The Journal of Cancer Research (1916–1930) | The American Journal of Cancer (1931–1940)

AACR American Association for Cancer Research

BRCA1 Deficiency Upregulates NNMT, Which Reprograms Metabolism and Sensitizes Ovarian Cancer Cells to Mitochondrial Metabolic Targeting Agents

Arun Kanakkanthara, Kiran Kurmi, Thomas L. Ekstrom, et al.

Cancer Res 2019;79:5920-5929. Published OnlineFirst October 16, 2019.